# Electron spin decoherence of single nitrogen-vacancy defects in diamond

J. R. Maze,[1] J. M. Taylor,[2] and M. D. Lukin[1]
[1]*Department of Physics, Harvard University, 17 Oxford Street, Cambridge, Massachusetts 02138, USA*
[2]*Department of Physics, Massachusetts Institute of Technology, 77 Massachusetts Avenue, Cambridge, Massachusetts 02138, USA*
(Received 29 April 2008; revised manuscript received 20 August 2008; published 23 September 2008)

We present a detailed theoretical analysis of the electron spin decoherence in single nitrogen-vacancy defects in ultrapure diamond. The electron spin decoherence is due to the interactions with $^{13}$C nuclear spins in the diamond lattice. Our approach takes advantage of the low concentration (1.1%) of $^{13}$C nuclear spins and their random distribution in the diamond lattice by an algorithmic aggregation of spins into small, strongly interacting groups. By making use of this *disjoint cluster* approach, we demonstrate a possibility of nontrival dynamics of the electron spin that cannot be described by a single time constant. This dynamics is caused by a strong coupling between the electron and few nuclei and exhibits large variations depending on the distribution of $^{13}$C nuclei surrounding each individual electronic spin. This results, in particular, in a substantial echo signal even at microsecond time scales. Our results are in good agreement with recent experimental observations.

DOI: 10.1103/PhysRevB.78.094303 PACS number(s): 03.65.Yz, 31.15.−p

## I. INTRODUCTION

Isolated spins in solid-state systems are currently being explored as candidates for good quantum bits, with applications ranging from quantum computation[1–3] and quantum communication[4] to magnetic sensing.[5–7] The nitrogen-vacancy (NV) center in diamond is one such isolated spin system. It can be prepared and detected using optical fields, and microwave radiation can be used to rotate the spin.[8,9] Recent experiments have conclusively demonstrated that in ultrapure diamond the electron spin coherence lifetime is limited by its hyperfine interactions with the natural 1.1% abundance carbon 13 in the diamond crystal.[10,11] Thus, developing a detailed understanding of the decoherence properties of such an isolated spin in a dilute spin bath is a challenging problem of immediate practical interest. This combined system of electron spin coupled to many nuclear spins has a rich and complex dynamics associated with many-body effects.

The decay of electronic spin coherence due to interactions with surrounding nuclei has been a subject of a number of theoretical studies.[12,13] Various mean-field and many-body approaches have been used to address this problem.[14–19] In this paper, we investigate a variation in the cluster expansion, developed in Ref. 16. Our approach takes advantage of the natural grouping statistics for randomly located, dilute impurities, which leads to the formation of small, disjoint clusters of spins which interact strongly within themselves and with the central spin, but not with other such clusters. This suggests a natural hierarchy of interaction scales of the system, and allows for a well-defined approximation that can be seen as an extension of ideas developed in the study of tensor networks.[20] We develop an algorithm for finding such clusters for a given set of locations and interactions, and find that for dilute systems convergence as a function of the cluster size (number of spins in a given cluster) is very rapid. We then apply this technique to the specific problem of the decay of spin echo for a single NV center and find good qualitative and quantitative agreements with experiments. In particular, we demonstrate a possibility of nontrival dynamics of the electron spin that cannot be described by a single time constant. This dependence is caused by a strong coupling between the electron and few nuclei and results in a substantial spin-echo signal even at microseconds time scale.

## II. METHODS

In this section, we introduce the properties of the electron spins in a NV center and the nuclear spins in its environment. Then, we address the many-body problem involved in the evaluation of spin-echo signals.

### A. Spin Hamiltonian

The negatively charged NV center ($[NV]^-$) has trigonal $C_{3v}$ symmetry and $^3A_2$ ground state[21] with total electronic spin $S=1$.[22] Spin-spin interaction leads to a zero-field splitting $\Delta=2.87$ GHz between the $m_s=0$ and $m_s=\pm 1$ manifolds, where the quantization axis is along the NV axis. This spin triplet interacts via hyperfine interaction with a spin bath composed of the adjacent nitrogen 14 and the naturally occurring 1.1% carbon 13 which is randomly distributed in the diamond lattice.

In the presence of an external magnetic field, the dynamics is governed by the following Hamiltonian:

$$H = \Delta S_z^2 - \gamma_e B_z S_z - \sum_n \gamma_N \mathbf{B}\cdot\mathbf{g}_n(|S_z|)\cdot\mathbf{I}_n + \sum_n S_z \mathbf{A}_n\cdot\mathbf{I}_n + \sum_n \delta\mathbf{A}_n(|S_z|)\cdot\mathbf{I}_n + \sum_{n>m}\mathbf{I}_n\cdot\mathbf{C}_{nm}(|S_z|)\cdot\mathbf{I}_m. \quad (1)$$

The relatively large zero-field splitting $\Delta$ [first term in Eq. (1)] does not allow the electron spin to flip and thus we can make the so-called secular approximation, removing all terms which allow direct electronic spin flips. Nonsecular terms have been included up to second order in perturbation theory, leading to the $|S_z|$ dependence of other terms in the Hamiltonian. The second and third terms are, respectively,

 

the Zeeman interactions for the electron and the nuclei, the fourth term is the hyperfine interaction between the electron and each nucleus, the fifth term is an effective crystal-field splitting felt by the nuclear spins, and the last term is the dipolar interaction among nuclei. The specific terms for this Hamiltonian are discussed in the Appendix.

For the case of the NV center, the nuclear $g$ tensor $\mathbf{g}_n$ can be anisotropic and vary dramatically from nucleus to nucleus.[11] This leads to a nontrivial dynamics between the electron and an individual nucleus (electron-nuclear dynamics) and motivates a new approach for the case of a dilute bath of spins described below. In addition, the interaction between nuclei is enhanced by the presence of the electron of the NV center. The resulting effective interaction strength can exceed several times the bare dipolar interaction between nuclei.[23]

### B. Disjoint cluster method: the idea

The large zero-field splitting $\Delta$ sets the quantization axis (called NV axis) and allows us to neglect electron spin flips due to interactions with nuclei. Therefore, we can reduce the Hilbert space of the system by projecting Hamiltonian (A3) onto each of the electron spin states. We can write the projected Hamiltonian, $P_{m_s} H P_{m_s}$ (where $P_{m_s} = |m_s\rangle\langle m_s|$) as

$$H_{m_s} = \sum_n \mathbf{\Omega}_n^{(m_s)} \cdot \mathbf{I}_n + \sum_{nm} \mathbf{I}_n \cdot \mathbf{C}_{nm}^{(m_s)} \cdot \mathbf{I}_m + \Delta |m_s| - \gamma_e B_z m_s, \tag{2}$$

where $m_s$ denotes the electron spin state, $\mathbf{\Omega}_n$ is the effective Larmor vector for nucleus $n$, and $\mathbf{C}_{nm}$ is the effective coupling between nuclei $n$ and $m$. In Eq. (2), we include the zero-field splitting and the Zeeman interaction. These terms provide just static fields whose effect is canceled by spin echo. In this way, we can write the evolution of the bath as $U_{m_s}(\tau) = T\{\exp(\int_0^\tau H_{m_s}(t')dt')\}$. An exact expression for $U_{m_s}$ can be found by ignoring the intrabath interactions ($\mathbf{C}_{nm} = 0$). However, for an interacting bath (with arbitrary $\mathbf{C}_{nm}$), solving $U_{m_s}$ for a large number of nuclei $N$ is a formidable task since it requires describing dynamics within a $2^N$ dimensional Hilbert space. Therefore, some degree of approximation is needed.

The spin bath considered here is composed of randomly distributed spins, and not all pair interactions among nuclei are equally important. Specifically, interactions decay with a characteristic law $1/R_{mn}^3$, where $R_{nm}$ is the distance between nuclei $n$ and $m$. As a result, we can break the big problem into smaller ones by grouping those nuclei that strongly interact with each other into disjoint sets. Our procedure is illustrated in Fig. 1. We denote the $k$th group of nuclei as $\mathcal{C}_g^k$, where the subindex $g$ indicates that each group has no more than $g$ nuclei. Interactions inside each group (intragroup interactions) are expected to be much larger than interactions among groups (intergroup interactions). Our approximation method will rely on neglecting the latter.

Formally, we start by separating intragroup interactions and intergroup interactions. We define the operator $H_B = \Sigma_k H(\mathcal{C}_g^k)$ which contains all electron-nuclear interactions

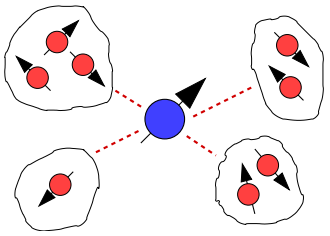

FIG. 1. (Color online) Illustration of the method. Spins that strongly interact can be grouped together and treated as isolated systems. Interactions that joint different groups can be incorporated as a perturbation.

[first term in Eq. (2)] plus all interactions between bath spins within the same group $\mathcal{C}_g^k$. Similarly, operator $H_A = H(\tilde{\mathcal{C}}_g) \times (= H - H_B)$ contains all interactions between bath spins in different groups. As a first approximation, we can neglect the intergroup interactions but keep the intragroup interactions. The approximation can be understood by means of the Trotter expansion[24]

$$\exp(H_A t + H_B t) = \lim_{x\to\infty} [\exp(H_A t/n)\exp(H_B t/n)]^n.$$

Since $H_B$ contains groups of terms that are disconnected from each other, $[H(\mathcal{C}_g^k), H(\mathcal{C}_g^{k'})] = 0$ and we can write the evolution operator as

$$U_g(\tau) = \lim_{x\to\infty} \left[ U\left(\tilde{\mathcal{C}}_g, \frac{\tau}{n}\right) \prod_k U\left(\mathcal{C}_g^k, \frac{\tau}{n}\right) \right]^n, \tag{3}$$

where $U(\tilde{\mathcal{C}}_g, \frac{\tau}{n})$ is the evolution operator due to Hamiltonian $H(\tilde{\mathcal{C}}_g)$ and so on.

To the zeroth order we neglect all terms in $H_A$ since $H(\tilde{\mathcal{C}}_g)$ contains interactions among nuclei that interact weakly. Thus, we set $U(\tilde{\mathcal{C}}_g, \frac{\tau}{n})$ to the identity and simplify Eq. (3) to

$$U_g(\tau) \approx \prod_k U(\mathcal{C}_g^k, \tau). \tag{4}$$

This approximation requires independent calculation of propagators for each group $g$, which corresponds to $N/g$ independent calculations of $2^g \times 2^g$ matrices, exponentially less difficult than the original problem of direct calculation of the $2^N \times 2^N$ dimensional matrix. We remark that including the effect of $U(\tilde{\mathcal{C}}_g, \frac{\tau}{n})$ in the Trotterization can be done by using a tree tensor network ansatz wave function[20] where the number of complex coefficients to describe the wave function is $O(N^{\log(N)})$ instead of $2^N$.

## III. ELECTRON SPIN ECHO

Electron spin echo removes static magnetic shifts caused by a spin bath, allowing the measurement of the dynamical changes in the bath. Assuming that an initial state $|\varphi\rangle = (|0\rangle + |1\rangle)/\sqrt{2}$ is prepared, the probability of recovering the same state after a time $2\tau$ is

$$p = \mathrm{Tr}[P_\varphi U_T(\tau)\rho U_T^\dagger(\tau)], \tag{5}$$

where $P_\varphi = |\varphi\rangle\langle\varphi|$ is the projector operator to the initial state, $\rho = |\varphi\rangle\langle\varphi| \otimes \rho_n$ is the density matrix of the total system, $\rho_n$ is the density matrix of the spin bath, $U_T(\tau) = U(\tau)R_\pi U(\tau)$ is the total evolution of the system where $U$ is the evolution operator under Hamiltonian (1), and $R_\pi$ is a $\pi$ pulse acting on the subspace $m_s = \{0,1\}$ of the electron spin manifold. Probability (6) can also be written as $p = [1 + S(\tau)]/2$, where

$$S(\tau) = \mathrm{Tr}[\rho_n U_0^\dagger(\tau) U_1^\dagger(\tau) U_0(\tau) U_1(\tau)] \tag{6}$$

is known as the pseudospin and $|S(\tau)| = 0$ is the long-time (completely decohered) signal. In the high-temperature limit, the density matrix of the nuclei can be approximated by $\rho_n \approx \mathbb{1}^{\otimes N}/2^N$, where $N$ is the number of nuclei. The generalization of this relation for different sublevels of the triplet state is straightforward $S(\tau) = \mathrm{Tr}[\rho_n U_\alpha^\dagger(\tau) U_\beta^\dagger(\tau) U_\alpha(\tau) U_\beta(\tau)]$, where $\alpha = 1$ and $\beta = -1$, for example. In what follows, we analyze the effect of an interacting bath on Eq. (6).

### A. Noninteracting bath

To understand the effect of an interacting bath we will first analyze the noninteracting case, which displays the phenomenon of electron spin–echo envelope modulation due to electron spin–nuclear spin entanglement. This is completely neglecting interactions among nuclei $\mathbf{C}_{nm} = 0$. In this regime, the evolution operator is factored out for each nucleus and the pseudospin is the product of all single pseudospin relations. In the high-temperature limit $\rho_n = \mathbb{1}/2$, we obtain the exact expression[11]

$$S_T(\tau) = \prod_n S_n(\tau) = \prod_n \left(1 - 2|\hat{\Omega}_n^{(0)} \times \hat{\Omega}_n^{(1)}|^2 \times \sin^2\frac{\Omega_n^{(0)}\tau}{2}\sin^2\frac{\Omega_n^{(1)}\tau}{2}\right). \tag{7}$$

When the electron spin is in its $m_s = 0$ state and the external magnetic field points parallel to the NV axis, the Larmor frequency $\Omega_n^{(0)}$ is set by the external magnetic field, and the nuclei precess with the same frequency $\Omega^{(0)}$. The total pseudospin is 1 at times $\Omega^{(0)}\tau = 2m\pi$ with $m$ integer. When the electron is in its $m_s = 1$ state, the Larmor vector $\mathbf{\Omega}_n^{(1)}$ has a contact and dipolar contribution from the hyperfine interaction $\mathbf{A}_n$ that may point in different directions depending on the position of the nucleus. As a consequence, when interactions from all nuclei are considered, these electron-nuclear dynamics makes the total pseudospin relation collapse and revive. However, it does not show any decay of the revival peaks.

We point out that when the transverse (perpendicular to the NV axis) magnetic field is nonzero, nuclei near the center experience an enhancement in their $g$ factors leading to a position-dependent Larmor frequency $\Omega_n^{(0)}$ (see the Appendix). This will result in an effective decay of the signal since the electron state will not be refocused at the same time for all nuclei.

### B. Interacting bath: an example

When the intrabath interactions are considered, the spin-echo signal can show decay in addition to the electron-nuclear dynamics. As an illustrative and simple example, consider a pair of nuclei with their Larmor vectors pointing in the same direction regardless of the electron spin state [in this case there is no electron-nuclear dynamics and the noninteracting pseudospin relation for two nuclei is $S_{nm} = S_n S_m = 1$ see Eq. (7)]. When the interaction between nuclei is included, the pseudospin relation can be worked out exactly

$$S_{nm}(\tau) = 1 - \left[\frac{\Delta\Omega_{nm}^0 c_{nm}^1 - \Delta\Omega_{nm}^1 c_{nm}^0}{2}\right]^2 \times \frac{\sin^2(\omega_{nm}^0\tau)\sin^2(\omega_{nm}^1\tau)}{(\omega_{nm}^0)^2(\omega_{nm}^1)^2}, \tag{8}$$

where $(\omega_{nm}^{m_s})^2 = (\Delta\Omega_{nm}^{m_s}/2)^2 + (c_{nm}^{m_s})^2$, $\Delta\Omega_{nm}^{m_s} = \Omega_n^{m_s} - \Omega_m^{m_s}$, and $c_{nm}^{m_s}$ is the strength of the dipolar interaction $c_{nm}^{m_s}(\hat{I}_{n+}\hat{I}_{m-} + \hat{I}_{n-}\hat{I}_{m+} - 4\hat{I}_{nz}\hat{I}_{mz})$ between nuclei $n$ and $m$. The two frequencies involved in Eq. (8) $\omega_{nm}^0$ and $\omega_{nm}^1$ are not necessarily the same for different pairs of nuclei. They depend on the relative position between nuclei and the relative position of each nucleus to the NV center. Therefore, when all pair interactions are included the pseudospin relation decays. In Sec. IV we present an approach to incorporate not only this two-body interaction but also $n$-body interactions with $n \leq 6$.

## IV. APPLICATION OF THE DISJOINT CLUSTER APPROACH

The many-body problem can be readily simplified by following the approximation described in Sec. II B. When the interactions that connect different groups are neglected, the evolution operator is factored out in groups and the spin-echo relation becomes simply

$$S_g(\tau) \approx \prod_k S(\mathcal{C}_g^k, \tau), \tag{9}$$

where $S(\mathcal{C}_g^k, \tau)$ is the pseudospin relation, Eq. (6), for group $\mathcal{C}_g^k$. $S_g(\tau)$ can be calculated numerically and exactly for small $g$ ($\leq 10$). Therefore, electron-nuclear and intrabath Hamiltonians can be simultaneously considered.

In Sec. IV A, we present our algorithm for sorting strongly interacting nuclei in a random distributed spin bath into well-defined groupings. We take the electron spin–echo signal, with the initial state $|\phi\rangle = (|0\rangle + |1\rangle)/\sqrt{2}$ as a figure of merit. We examine the convergence of our disjoint cluster approach as a function of the maximum group size $g$ and consider the statistics of spin echo for a variety of physical parameters such as carbon 13 abundance and magnetic-field magnitude and orientation.

### A. Grouping algorithm

One of the criteria to aggregate groups of spins is to consider the strength of the intrabath interaction. This parameter can be summarized in one variable $\mathbb{C}(i,j)$ which is a scalar function of the interaction $\mathbf{C}^{ij}$ between nuclei $i$ and $j$. The

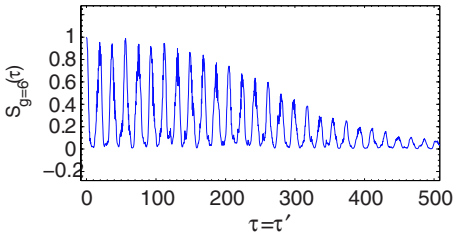


FIG. 2. (Color online) Simulation of the pseudospin $S_{g=6}(\tau)$ for a single NV center in a magnetic field of 50 Gauss oriented parallel to the NV axis.

aggregation algorithm used for this criterion is as follows. Consider an array $\mathbb{A}$ containing the criterion for all pairs ordered from high to low values in $\mathbb{C}$ and let $\{i,j\}_n$ be the $n$th nuclear pair in array $\mathbb{A}$. The array $\mathbb{A}$ is scanned completely and one of the following cases applies for each pair $\{i,j\}_n$: (i) if nuclei $i$ and $j$ belong to different groups, join both groups if $\mathcal{N}[\mathbb{G}(i)]+\mathcal{N}[\mathbb{G}(j)]\leq g$; (ii) if nucleus $i$ belongs to group $\mathbb{G}(i)$ and nucleus $j$ does not belong to any group, add $j$ to group $\mathbb{G}(i)$ if $\mathcal{N}[\mathbb{G}(i)]<g$. If not, make a new group with $j$; (iii) if nucleus $j$ belongs to group $\mathbb{G}(j)$ and nucleus $i$ does not belong to any group, add $i$ to group $\mathbb{G}(j)$ if $\mathcal{N}[\mathbb{G}(j)]<g$. If not, make a new group with $i$; (iv) if nuclei $i$ and $j$ do not belong to any group, make a new group with $i$ and $j$, where $\mathcal{N}(\mathbb{G})$ is the number of nuclei in group $\mathbb{G}$ and $g$ is the maximum number of nuclei per group. In what follows, we use the criterion $\mathbb{C}(i,j)=(C_{xx}^{ij})^2+(C_{yy}^{ij})^2+(C_{zz}^{ij})^2$ (i.e., the interaction between nuclei $i$ and $j$) to estimate the electron spin echo in NV centers.

### B. Numerical methods and example cases

In the particular case of the NV center, the interaction between nuclei $\mathbf{C}^{ij}$ involves both the bare dipolar interaction and a second-order process interaction mediated by the electron spin (see the Appendix). The latter interaction does not depend on the distance between nuclei but rather on the distance between each nuclei and the electron. As a result, it can couple two separate nuclei that are near the electron but far from each other. At low fields ($<1000$ Gauss), these second-order processes are reduced by the large zero-field splitting $\Delta$ ($\approx 3$ GHz) and by the large average distance between nuclei [hundred times the nearest-neighbor distance $100\times 1.54$ Å at the natural abundance of $^{13}$C (1.1%)]. In this regime, the dynamics can be faithfully described by considering a small number of nuclei ($\leq 6$) near the electron spin in a single group.

Figure 2 shows $S_g(\tau)$ for $g=6$ [Eq. (9)] for 750 random and distributed carbon 13 in a diamond lattice in a magnetic field of 50 Gauss oriented along the NV axis. The algorithm was implemented using MATLAB and the Hamiltonian for each group was diagonalized exactly followed by the calculation of the corresponding unitary matrices for 6000 points from 0 to 1 ms. Each simulation of $S_g(\tau)$ takes approximately 10 min.

The method also shows good convergence. When the maximum size of subgroups $g$ is increased, more interactions among nuclei are considered and the approximation gets better. As a figure of merit, we plot the integrated squared difference between consecutive spin-echo relations $S_g$ and $S_{g-1}$,

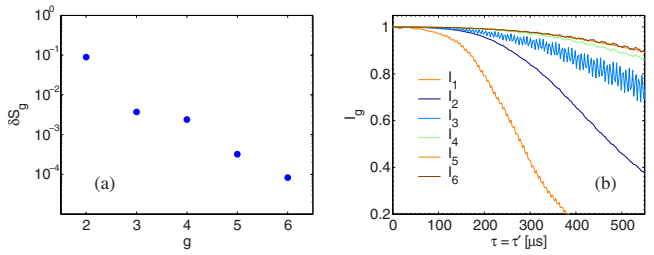


FIG. 3. (Color online) (a) Convergence: Eq. (11) as the maximum number of nuclei $g$ per group is increased. (b) Indicators $I_g$ of the contribution of neglected pairs. When $g$ is increased, the most important pair interactions are added to the pseudospin relation $S_g$. The rest is used to calculate $I_g$.

$$\langle \delta S_g^2 \rangle = \frac{1}{T}\int_0^T [S_g(t) - S_{g-1}(t)]^2 dt. \tag{10}$$

Figure 3(a) shows $\frac{1}{2}\log\langle \delta S_g^2 \rangle$ up to $g=6$. Each time the maximum size $g$ of subgroups $\mathcal{C}_g^k$ is increased, the spin-echo relations $S_g$'s get closer.

In addition, following Ref. 16, we introduce the following indicator of all interactions not included in groups $\mathcal{C}_g^k$ and therefore in $S_g$:

$$I_g(\tau) = \prod_{\{n,m\}\in\tilde{\mathcal{C}}_g} S_{nm}(\tau). \tag{11}$$

The product in Eq. (11) runs over all neglected pair interactions contained in $\tilde{\mathcal{C}}_g$ and $S_{nm}$ is calculated according to Eq. (8). In this way, $I_g(\tau)$ has the next order of smallest couplings for a given spin bath distribution and is an indicator of convergence for our approach that obeys $0\leq I_g(\tau)\leq 1$. When $I_g(\tau)$ is close to unity, good convergence is achieved. Figure 3(b) shows $I_g(\tau)$ for several aggregations (different $g$'s). As expected, when the maximum subgroup size $g$ is increased, the contribution from all neglected interactions is small. By the time the neglected interactions become important, the pseudospin $S_g(\tau)$ has already decayed (see Fig. 2).

## V. RESULTS AND DISCUSSION

The results shown in Fig. 4 clearly indicate that the electron spin–echo signal cannot be modeled by just one time scale. This result can be understood by noting that few strongly interacting nuclei can coherently modulate the usual exponential decay. This is in good quantitative agreement with recent experimental results.[6]

The random distribution of the spin bath and the relative high coupling between two nearest-neighbor nuclei ($\sim 2$ kHz) may cause a few nuclei to contribute significantly to the decay of the spin-echo signal. Nuclei that makes small contributions to the decoherence of the electron contribute as $1-a\tau^4\approx\exp(-a\tau^4)$ as it can be seen from Eq. (8). This behavior starts to deviate from $\exp(-a\tau^4)$ as the interaction between nuclei increases. Figure 4(a) shows a very unusual

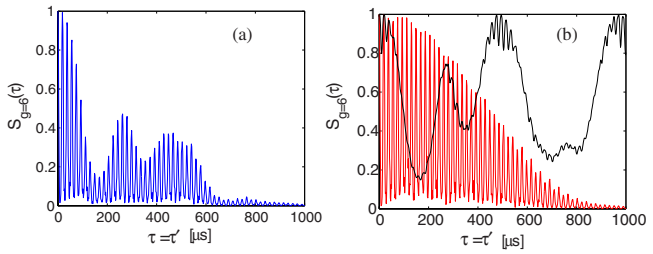


FIG. 4. (Color online) (a) Electron spin–echo signal highly modulated by a few carbon 13 that strongly interact with the electron spin. (b) The strong contribution to the signal (black curve) has been isolated from the contribution from the rest of the spin bath (red curve).

decay at which few nuclei modulate coherently [Fig. 4(b), black curve] the irreversible contribution from the rest of the bath [Fig. 4(b), red curve]. Therefore, individual NV centers can show a rich variety of spin-echo signals with multiple time scales. The coherent modulation of the spin-echo diffusion due to strong interacting nuclei suggests that we can think about a system composed of the electron and these few strong interacting nuclei and an environment composed of the rest of the spin bath.

Each NV center experiences a different random configuration and concentration of carbon 13. This causes a large distribution of decoherence times $T_2$ when many centers are probed. In order to estimate the decoherence time $T_2$ we fit the envelope of $S_g(\tau)$ to $\exp[-(2\tau/T_2)^3]$. When the fit is not accurate we define $T_2$ as the longest time for which $S_g \geq 1/e$. Figure 5(a) shows the histogram of $T_2$ for 1000 different random distributions of carbon 13 in the diamond lattices for an external magnetic field of 50 Gauss parallel to the NV axis. Clearly, there exists substantial variation in $T_2$ for different centers.

As expected, the decoherence time decreases as the impurity concentration increases. This is shown in Fig. 5(b) where $T_2$ goes as $1/n$. To understand this it is possible to make an analysis using a small $\tau$ expansion; while this is not always correct, it provides a simple explanation of the underlying behavior. From Eq. (8), the decoherence time scales as the geometric mean of the bath dynamics and the bath-spin interaction, i.e., $T_2 \sim (\bar{C}A_c)^{-1/2}$, where $\bar{C}$ is the averaged nuclear-nuclear dipolar interaction and $A_c$ is some characteristic value for the electron-nuclear interaction. Since both

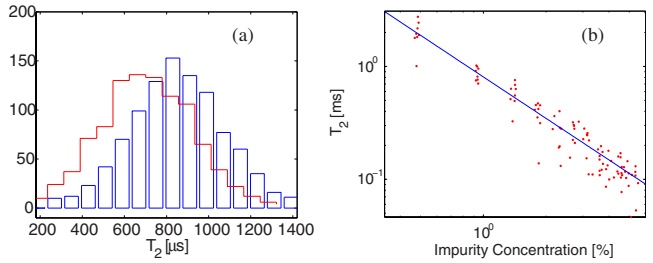


FIG. 5. (Color online) Histogram of $T_2$ for 1000 simulations at a magnetic field of 50 Gauss at an angle of $\theta=0°$ (blue) and $\theta=6°$ (red) with respect to the NV axis. (b) Decoherence time $T_2$ versus impurity concentration, carbon 13, at 50 Gauss along the NV axis.

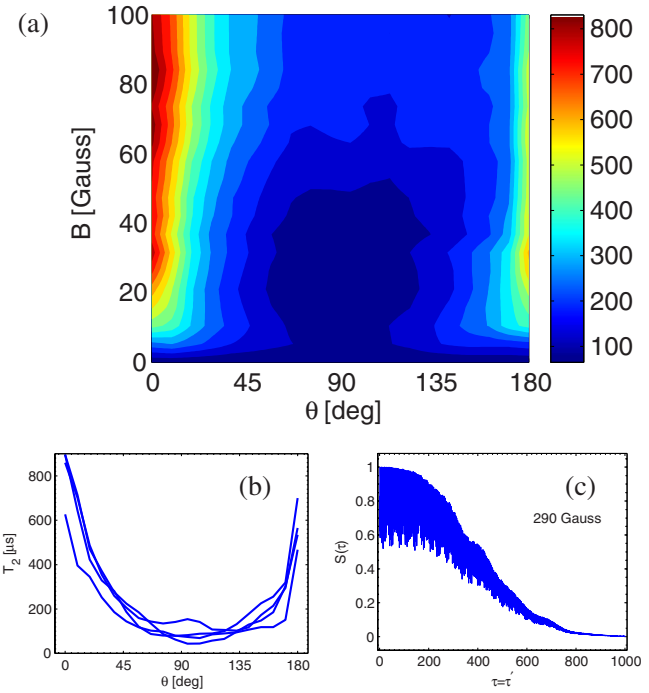


FIG. 6. (Color online) (a) Coherent time $T_2$ for different magnetic-field strength and angles (measured from the NV axis). Each point is the average of over six different random distributed baths. (b) Coherence time $T_2$ versus angle of the magnetic field for four different spin baths at 50 Gauss. (c) Pseudospin $S_{g=6}(\tau)$ at 290 Gauss. At high fields the collapses due to the electron-nuclear dynamics decrease (see text).

interactions decay as $r^{-3}$ and the average distance between bodies scales with the concentration as $n^{-1/3}$, both interactions scale linearly in $n$. Therefore, the decoherence time $T_2$ decreases approximately as $1/n$.

For nonzero transverse magnetic fields, second-order processes via the electron spin (see Appendix) make a substantial contribution to decoherence. Even in the case of noninteracting nuclei, Eq. (7), a transverse magnetic field causes the revivals to diminish due to an enhanced nuclear $g$ factor experienced by nuclei near the electron [see Eq. (A4)]. To understand this effect, consider that revivals occur because in each half of the spin-echo sequence each $^{13}$C nuclear spin makes a full $2\pi$ Larmor precession (or multiples of it). Thus, in each half of the spin-echo sequence the accumulated Zeeman shift, due to the ac component of the $^{13}$C nuclear field, cancels regardless of the initial phase of the oscillating field produced by the $^{13}$C nuclear spins. The $^{13}$C nuclear dc field component is refocused by spin echo. However, if different nuclei precess at different Larmor frequencies $\Omega_n^0$, the accumulated Zeeman shifts for each nuclei cancel at different times and therefore the total accumulated Zeeman shift will be nonzero, preventing a complete refocusing of the electron spin. In addition, the average interaction between nuclei close to the electron spin is enhanced due to the enhancement of their $g$ factors [see Eq. (A4)]. These effects are illustrated in Fig. 5(a) for a magnetic field at an angle of $\theta=6°$ from the NV axis and in Fig. 6(b).

As the angle between the magnetic field and the NV axis $\theta$ is increased, the electron-nuclear dynamics dominates and

the spin-echo signal shows small revivals and fits poorly to a single exponential decay. Thus, to describe the coherence time at these angles, we have plotted the average value of the signal normalized by the average signal at $\theta=0°$:[25]

$$T_2(B,\theta) \equiv T_2(B,\theta=0)\frac{\int_0^\infty |S_{B,\theta}(t)|dt}{\int_0^\infty |S_{B,\theta=0}(t)|dt}. \quad (12)$$

Figure 6(a) shows how the coherence of the signal varies with the strength and orientation of the magnetic field. This map is the average of over six different spin baths, since the random localization of carbon 13 nuclei in the lattice makes the coherent time to vary from NV center to NV center as it can be seen in Fig. 6(b) for a fixed magnetic field.

When the magnetic field along the NV axis increases, the contribution from the electron-nuclear interactions decreases [see Fig. 6(c)]. This happens because the quantization axis for the nuclei points almost in the direction of the external magnetic field producing a small oscillating field. This can be easily seen in the noninteracting case, Eq. (8), where the second term vanishes if $\mathbf{\Omega}_n^{(0)} \| \mathbf{\Omega}_n^{(1)}$. Similarly, when electron spin echo is performed using the submanifold $m_s=\{+1,-1\}$, the signal does not revive since each nucleus refocuses the electron at different times. This occurs because the Larmor frequencies in this case $\Omega_n^{\pm 1}$ are position dependent and differ for each nucleus.

We also point out that the approximation introduced in Sec. II B is valid as long as the impurity concentration of carbon 13 is not too high, so the neglected interactions that connect different groups do not play an important role. This allows us to treat the bath as isolated group. A heuristic argument to evaluate the validity of the present method is to consider the ratio between intra- and intergroup dipolar integrations. We consider the root mean square (RMS) value of the dipolar interaction since the interaction itself average to zero due to its angular dependence when an isotropic distribution of nuclear spins is considered and due to the random initial spin configuration in the high-temperature limit. The RMS contribution from a shell of spins is proportional to $I(r_{\min},r_{\max})=(\int_{r_{\min}}^{r_{\max}} r^{-6} 4\pi r^2 dr)^{1/2}=[(4\pi/3)(r_{\min}^{-3}-r_{\max}^{-3})]^{1/2}$. Therefore, the ratio between intra- and intergroup interactions can be estimated as $I(r_{nn},r_g)/I(r_g,R)\approx(r_g/r_{nn})^{1/2}$, where $r_{nn}$ is the nearest-neighbor distance, $r_g$ is the radius of the group that contains $g$ nuclear spins, and $R$ is the radius of the spin bath. For a given concentration of carbon 13 $n$, the number of nuclear spins $g$ inside a sphere of radius $r_g$ is $g=n\times 8\times 4\pi(r_g/a)^3/3$, where $a$ is the size of the unit cell which contains eight carbons. Under these considerations, the mentioned ratio is $\sqrt{g/nN_{nn}}\approx\sqrt{g/4n}$, where $N_{nn}$ is the number of carbons inside a sphere of radius $r_{nn}$ for which we have assigned a conservative value of 4. For the concentration of carbon 13 ($n\sim 1\%$), this ratio is much larger than one, supporting the validity of the current approximation. The approximation also relies on the relatively large interaction between the central spin (electron) and the bath $\mathbf{A}_n$ when compared to the intrabath interaction $\mathbf{C}_{nm}$. The reason for this is that as the central spin gets disconnected from the bath (reducing $\mathbf{A}_n$), the decay occurs at later times $\tau$ and interactions of the order of $\tau^{-1}$ start to play a role. To illustrate this, consider the size of each subgroup scaling as $(g/n)^{1/3}$, where $g$ is the size of the subgroup. Then, the interaction between nearest-neighbor groups scales as $nC_{nn}/g$, where $C_{nn}$ is the nearest-neighbor nuclear interaction. The time at which this interaction is important goes as $t\sim g/nC_{nn}=g/\bar{C}$. If we require this time to be larger than the decoherence time ($t\gg T_2$), we find that the two types of interactions should satisfy $g(A_c/\bar{C})^{1/2}\gg 1$ (for the present study this value is around 150). Therefore, when the interaction between the addressed spin and the bath is of the order of the intrabath interactions, the approximation breaks down. This would be the case of the spin-echo signal for a nuclear spin proximal to the NV center[23] in which more sophisticated methods should be applied such as tree tensor networks.[20]

## VI. CONCLUSIONS

We have presented a method to evaluate the decoherence of a single spin in the presence of an interacting randomly distributed bath. It properly incorporates the strong electron-nuclear dynamics present in NV centers and explains how it affects the decoherence. We also incorporate the dynamic beyond the secular approximation by including an enhanced nuclear $g$ factor that depends on the orientation of the external magnetic field relative to the NV axis and by including an electron mediated nuclei interaction. Our results show that the spin-echo signal for NV centers can present multiple time scales where the exponential decay produced by many small nuclei contributions can be coherently modulated by few strongly interacting nuclei. The coherence times in ultrapure diamond can be further improved by making isotopically pure diamond with low concentration in carbon 13. This method may be used in other systems as long as the intrabath interaction is smaller than the interaction between the central spin and the bath. These results have important implications, e.g., in magnetometry where long coherence times are important. For example, echo signals persisting for up to milliseconds can be used for nanoscale sensing of weak magnetic fields, as it was demonstrated recently.[6]

## ACKNOWLEDGMENTS

The authors would like to thank S. Das Sarma for useful comments. This work was supported by NSF, DARPA, and the Packard foundation. J.R.M. thanks the Fulbright-Conicyt foundation for support. J.M.T. is supported by the Pappalardo Foundation.

## APPENDIX: HAMILTONIAN FOR NV CENTERS

Electron spin resonance shows that the nuclear spin–electron spin interaction is 150 MHz (Ref. 22) for the three nearest-neighbor carbon 13's and around 2 MHz for the nitrogen. Away from this deep defect, the interaction is dipolarlike

$$\mathbf{S}\cdot\mathbf{A}_n\cdot\mathbf{I}_n \equiv 5.6\left(\frac{a_{nn}}{R_n}\right)^3[3(\hat{S}\cdot\vec{n})(\hat{I}_n\cdot\vec{n})-\hat{S}\cdot\hat{I}_n]\ \text{MHz}, \tag{A1}$$

where $a_{nn}=1.54$ Å is the nearest-neighbor distance for diamond, $R_n$ is the distance between the $n$th carbon 13 and the defect, and $\vec{n}$ is the unit vector that connects the electron and the nucleus. Carbon 13's interact via dipolar interaction

$$\mathbf{I}_n\cdot\mathbf{C}_{nm}\cdot\mathbf{I}_m \equiv 2.1\left(\frac{a_{nn}}{R_{nm}}\right)^3[3(\hat{I}_n\cdot\vec{n})(\hat{I}_m\cdot\vec{n})-\hat{I}_n\cdot\hat{I}_m]\ \text{kHz}, \tag{A2}$$

where $R_{nm}$ is the distance between the $n$th and $m$th carbon 13.

Recent experiments have been performed at fields of 1–100 Gauss (Ref. 11) with Zeeman energies of megahertz and kilohertz for the electron and carbon 13 nuclear spins, respectively. At these fields, it is convenient to make the so-called secular approximation thanks to the large splitting $\Delta$. However, transverse directions (perpendicular to the NV axis) of the external magnetic field and hyperfine fields from carbon 13 must be taken into account as a perturbation to get an accurate description of the system, as it has been shown by experiments.[11] Including this, we can write the Hamiltonian in the following form:

$$\begin{aligned} H \approx{}& \Delta S_z^2-\gamma_e B_z S_z+\sum_{nj} S_z A_{zj}^n I_j^n+\sum_n \delta\mathbf{A}_n^{\mathrm{T}}\cdot\mathbf{I}_n \\ &-\gamma_N\sum_n \mathbf{B}^{\mathrm{T}}\cdot\mathbf{g}_n^{\mathrm{eff}}\cdot\mathbf{I}_n+\sum_{n>m}\mathbf{I}_n^{\mathrm{T}}\cdot\mathbf{C}_{nm}^{\mathrm{eff}}\cdot\mathbf{I}_m, \end{aligned} \tag{A3}$$

where $\mathbf{g}_n^{\mathrm{eff}}=1+\delta\mathbf{g}_n(m_s)$ is the effective $g$ tensor,[11] $\mathbf{C}_{nm}^{\mathrm{eff}}=\mathbf{C}_{nm}+\delta\mathbf{C}_{nm}(m_s)$ is the effective coupling between carbon 13's, and

$$\delta\mathbf{g}_n(m_s)=-\frac{(2-3|m_s|)\gamma_e}{\Delta\gamma_N}\begin{pmatrix} A_{xx}^n & A_{xy}^n & A_{xz}^n \\ A_{yx}^n & A_{yy}^n & A_{yz}^n \\ 0 & 0 & 0 \end{pmatrix},$$

$$\delta\mathbf{C}_{nm}(m_s)=-\frac{(\Delta\gamma_N/\gamma_e)^2}{\Delta(2-3|m_s|)}\delta\mathbf{g}_n^T\cdot\delta\mathbf{g}_m,$$

$$\delta\mathbf{A}_n^{\mathrm{T}}(m_s)=\frac{(2-3|m_s|)}{2\Delta}\sum_{ij}\epsilon_{ijk}A_{xi}^n A_{yj}^n. \tag{A4}$$

For nuclei close to the center, $\delta g$ can reach values between 0 and 15 (Ref. 11); $\delta C$ can be several times the bare dipole-dipole interaction.[23] The term $\delta A$ is a small contribution that can be neglected in most of the cases due to the large value of the zero-field splitting $\Delta$.


[1] B. E. Kane, Nature (London) **393**, 133 (1998).
[2] D. Loss and D. P. DiVincenzo, Phys. Rev. A **57**, 120 (1998).
[3] J. Wrachtrup and F. Jelezko, J. Phys.: Condens. Matter **18**, S807 (2006).
[4] L. Childress, J. M. Taylor, A. S. Sorensen, and M. D. Lukin, Phys. Rev. Lett. **96**, 070504 (2006).
[5] J. M. Taylor, P. Cappellaro, L. Childress, L. Jiang, D. Budker, P. R. Hemmer, A. Yacoby, R. Walsworth, and M. D. Lukin (unpublished).
[6] J. R. Maze, P. L. Stanwix, J. S. Hodges, S. Hong, J. M. Taylor, P. Cappellaro, L. Jiang, A. Zibrov, M. V. G. Dutt, E. Togan, A. S. Zibrov, A. Yacoby, R. L. Walsworth, and M. D. Lukin (unpublished).
[7] G. Balasubramanian, I.-Y. Chan, R. Kolesov, M. Al-Hmoud, C. Shin, C. Kim, A. Wojcik, P. R. Hemmer, A. Kruger, F. Jelezko, and J. Wrachtrup (unpublished).
[8] N. B. Manson, X.-F. He, and P. T. H. Fisk, Opt. Lett. **15**, 1094 (1990).
[9] F. Jelezko, T. Gaebel, I. Popa, M. Domhan, A. Gruber, and J. Wrachtrup, Phys. Rev. Lett. **93**, 130501 (2004).
[10] E. Van Oort and M. Glasbeek, Chem. Phys. **143**, 131 (1990).
[11] L. Childress, M. V. Gurudev Dutt, J. M. Taylor, A. S. Zibrov, F. Jelezko, J. Wrachtrup, P. R. Hemmer, and M. D. Lukin, Science **314**, 281 (2006).
[12] N. Shenvi, R. de Sousa, and K. B. Whaley, Phys. Rev. B **71**, 224411 (2005).
[13] W. A. Coish and D. Loss, Phys. Rev. B **70**, 195340 (2004).
[14] R. de Sousa and S. Das Sarma, Phys. Rev. B **67**, 033301 (2003).
[15] R. de Sousa and S. Das Sarma, Phys. Rev. B **68**, 115322 (2003).
[16] W. M. Witzel, R. de Sousa, and S. Das Sarma, Phys. Rev. B **72**, 161306(R) (2005).
[17] W. A. Coish and D. Loss, Phys. Rev. B **72**, 125337 (2005).
[18] W. Yao, R.-B. Liu, and L. J. Sham, Phys. Rev. B **74**, 195301 (2006).
[19] S. K. Saikin, W. Yao, and L. J. Sham, Phys. Rev. B **75**, 125314 (2007).
[20] Y.-Y. Shi, L.-M. Duan, and G. Vidal, Phys. Rev. A **74**, 022320 (2006).
[21] J. P. Goss, R. Jones, S. J. Breuer, P. R. Briddon, and S. Öberg, Phys. Rev. Lett. **77**, 3041 (1996).
[22] X.-F. He, N. B. Manson, and P. T. H. Fisk, Phys. Rev. B **47**, 8816 (1993).
[23] M. V. G. Dutt, L. Childress, L. Jiang, E. Togan, J. Maze, F. Jelezko, A. S. Zibrov, P. R. Hemmer, and M. D. Lukin, Science **316**, 1312 (2007).
[24] H. F. Trotter, Proc. Am. Math. Soc. **10**, 545 (1959).
[25] We choose this approach as the signal has sufficiently nontrivial electron-nuclear dynamics for $\theta\neq 0$ that fitting an envelope decay function, as is done for $\theta=0$, leads to large errors.